Title: A single nuclei transcriptomic analysis of the Atlantic salmon gill through smoltification and seawater transfer

Authors: Alexander C. West[1], Yasutaka Mizoro[2], Shona H. Wood[1], Louise Ince[3], Marianne Iversen[1], Even H. Jørgensen[1], Torfinn Nome[4], Simen Rød Sandve[4], Andrew S. I. Loudon[3] and David G. Hazlerigg[1]

[1]Arctic Chronobiology and Physiology, University of Tromsø, 9019 Tromsø, Norway

[2]Unit of Animal Genomics, GIGA Institute, University of Liège, Liège, Belgium

[3]University of Geneva, Centre Médical Universitaire (CMU), Department of Pathology and Immunology, Switzerland

[4]Centre for Integrative Genetics, Department of Animal and Aquaculture Sciences, Norwegian University of Life Sciences, 1432 Ås, Norway

[5]Division of Diabetes, Endocrinology & Gastroenterology, School of Medical Sciences, Faculty of Biology, Medicine and Health, University of Manchester, UK

*Correspondence: david.hazlerigg@uit.no

Abstract

Anadromous salmonids begin life adapted to the freshwater environments of their natal streams before a developmental transition, known as smoltification, transforms them into marine-adapted fish. In the wild, the extending photoperiods of spring stimulates smoltification, typified by radical reprogramming of the gill from an ion-absorbing organ to ion-excreting organ. Prior work has highlighted the role of specialized “mitochondrion-rich”

cells in delivering this phenotype. However, transcriptomic studies identify thousands of smoltification-driven differentially regulated genes, indicating that smoltification causes a multifaceted, multicellular change; but direct evidence of this is lacking.

Here, we use single-nuclei RNAseq to characterize the Atlantic salmon gill during smoltification and seawater transfer. We identify 20 distinct clusters of nuclei, including known, but also novel gill cell types. These data allow us to isolate cluster-specific, smoltification-induced changes in gene expression. We also show how cellular make-up of the gill changes through smoltification. As expected we noted an increase in the proportion of seawater mitochondrion-rich cells, however, we also identify a reduction of several immune-related cells. Overall, our results provide unrivaled detail of the cellular complexity in the gill, and suggest that smoltification triggers unexpected immune reprogramming directly preceding seawater entry.

Keywords: Atlantic salmon, smoltification, photoperiod, seasonal, gill

Introduction

The Atlantic salmon migrates between fresh and seawater environments [1]. Atlantic salmon eggs hatch in freshwater streams where they develop for 1-4 years. On reaching a critical size threshold, young “parr” animals are sensitized by several weeks of winter photoperiod (day-lengths), after which long, summer-like photoperiods stimulates the parr to transform into a marine-adapted “smolt” fish [2]. This process, known as smoltification, drives divergent expression of endocrine factors that collectively deliver phenotypic remodeling, of length, weight, silvering, and in particular: gill physiology [1].

44 The salmonid gill is a complex multifunctional organ, essential for gas exchange,
45 nitrogenous waste excretion, pH balance and osmoregulation [3]. It is also a major mucosal
46 immune barrier harboring a dedicated lymphoid tissue [4]. Structurally, the gills are arranged in
47 symmetrical arches, each of which are populated by numerous filament structures, which are
48 themselves densely flanked with lamellae. The gill is composed of seven major cell types [5].
49 Pavement cells (PVCs) have an enlarged surface area on the apical membrane, and form the
50 majority of the epithelium [6]. Pillar cells (PCs), which are structural cells, define the blood
51 spaces within the lamellae [7]. Goblet cells (GCs) reside in the filament epithelium and excrete
52 mucus [8]. Non-differentiated progenitor cells (NDCs) colonize basal and intermediate layers of
53 the gill epithelium [9]. Chemosensory neuroepithelial cells (NECs) lie along the length of the
54 efferent edge of the gills and are innervated by the central nervous system [10]. Mitochondrion-
55 rich cells (MRCs) and their adjacent accessory cells (ACs), finally, are located at the trough
56 between two lamellae where they abundantly express the channels and pumps required to
57 maintain the osmotic gradients between blood plasma and both fresh- and seawater [11–13].

58 Under freshwater, Na^+ ions are directly or indirectly exchanged for protons across the
59 apical membrane then transported into the blood *via* the sodium potassium ATPase (NKA) on
60 the basolateral membrane [14–16]. Cl^- ions, meanwhile, are exchanged or channeled across the
61 apical membrane then enter the blood [17–20]. Under saltwater, basolateral NKA generates a
62 chemical and electrical gradient, motivating both loss of Cl^- ions *via* apical CFTR channels and
63 paracellular escape of Na^+ ions [13,21] (reviewed in [22]).

64 Smoltification converts the Atlantic salmon gill from a freshwater-adapted organ to a
65 seawater-adapted organ. Rising cortisol and growth hormone along with falling prolactin
66 propels smoltification. This change in endocrinology coincides with a switch in anatomical and

67 molecular phenotypes of MRCs and ACs, cell types which to date comprise the major focus of
68 smoltification of gill physiology [1,12,23]. Smoltification is, however, a complex developmental
69 transition and the smolt gill phenotype likely extends far beyond changing MRC and AC cell
70 phenotype. Therefore, to realize the complexities of smoltification-driven changes in gill
71 physiology we adopt a new strategy, single-nuclei RNAseq, which provides transcriptional
72 responses to smoltification and seawater transfer at individual nuclei-level resolution.

73 **Results & Discussion**

74 **A single-nuclei survey of Atlantic salmon gill cells**

75 We profiled 18,844 individual nuclei from eight Atlantic salmon gill samples from four distinct
76 physiological states (Figure 1A). To define shared correlation structure across datasets we
77 pooled replicate samples and integrated all four states using diagonalized canonical
78 correlation analysis followed by L2 normalization. We next identified pairs of mutual nearest
79 neighbors (MNNs) to identify anchors: cells that represent shared biological states across
80 datasets. Anchors were then used to calculate "correction" vectors allowing all fours states to
81 be jointly analyzed as an integrated reference [24]. Unsupervised graph clustering partitioned
82 the nuclei into 20 clusters, which we visualized using a uniform manifold approximation and
83 projection (UMAP) dimension reduction technique (Figure 1B).

84 Lists of co-expressed marker genes define individual clusters. We categorized
85 individual clusters using gene ontology analysis of marker gene lists and unique expression of
86 known marker genes. This approach allowed us to infer cell types including fresh- and
87 seawater MRCs, ACs, neuroepithelial cells, goblet cells, non-differentiated cells, pillar cells,
88 lymphoid endothelial cells and several types of blood cell. We also identified a novel
89 population of fibrocyte-like cells, and several types of vascular- and endothelial-like cells that

90 partitioned across several clusters, together suggesting greater complexity in gill cytology that
91 previously appreciated (Figure 1B).

92 We then defined expression signatures for each cell cluster. Our analysis re-identified
93 several known marker genes, but also identifying several novel cell-type markers (Figure 1C).
94 For example, the accessory cell signature included highly restricted expression of Slc26a6, an
95 apical membrane Cl^-/HCO_3 exchanger, associated with gill function but until now
96 misattributed to expression within MRCs [25,26]. We were interested to note that the markers
97 defining the erythrocyte population, including beta-globin, were expressed widely among all
98 cell types. It is unclear exactly what role extra-erythroid haemoglobin plays in the gill,
99 however, mammalian studies suggest that haemoglobin, in addition to its oxygen carrying
100 capacity, may play an antimicrobial role [27]. As a major mucosal immune barrier, this capacity
101 may be pertinent to the gill [28].

102 **Major changes in cell composition during smoltification**

103 To understand how gene expression and cellular complexity changes within the gill during
104 smoltification and seawater transfer we compared the snRNAseq profiles at different
105 developmental points (Fig 2A, for confirmation of smolt status see[29]). The abundance of six
106 nuclei clusters changed dramatically (>3 fold change in percentage abundance) during
107 smoltification (Figure 2B). SW MRCs increased in proportion steadily from T1-T4, consistent
108 with previous descriptions of Atlantic salmon gill physiology. We also observed a marked
109 increase in vascular cell number, with the major differences occurring between T2 and T3,
110 suggesting that this vascular cell cluster proliferate in line with growth rates (Figure 2C).
111 Interestingly, four immune-related nuclei clusters representing T cells, myeloid cells, dendritic
112 cells and lymphatic endothelial cells fell dramatically during smoltification (Figure 2D).

113 Changes in cell abundance occurred with a similar profile in all immune-associated cell
114 clusters, with consistent decline observed between T1-T3. In contrast, 24h SW transfer does
115 not appear to affect immune-cell abundance directly. These results highlight the complex and
116 dynamic changes in cellular composition that occur in the gill during smoltification.

117 **Cell cluster-specific expression of smoltification-associated factors**

118 Next, we wanted to identify cluster types where smoltification drives changes in local gene
119 regulation. For statistical power, we cross-referenced our snRNAseq analysis with whole gill
120 RNAseq analysis of T1-T3, identifying 9746 genes differentially regulated by smoltification
121 (FDR <0.01). Pearson clustering of these genes resolved five major clusters that were
122 associated with immune response, structural morphogenesis, autophagy, catabolism and
123 mitochondrial respiration (Figure 3A). Within our analysis we identified a number of "classical"
124 smoltification-related genes. As expected, CFTR was highest under constant light (LL), and was
125 highly localized in expression to MRCs (Figure 3B). We also identified the reciprocal regulation
126 of sodium-potassium ATPase subunits, specifically, suppression of NKAa1a and increase in
127 NKAa1b [12]. Inspection of cellular localization within our snRNAseq dataset showed that
128 expression of these genes were, as anticipated, highest within the MRCs and ACs (Figure 3B).

129 Our previous work identified genes whose expression are predicated on exposure to
130 several weeks of short-photoperiod exposure[29]. In Atlantic salmon, these "winter-dependent"
131 genes are analogous to vernalization dependent genes in *Arabidopsis*[30], where a dosage of
132 exposure to a winter-like stimulus (in *Arabidopsis*, cold; in Atlantic salmon, short phootperiod)
133 controls the presentation of a seasonal phenotype under summer-like stimulus (in
134 *Arabidopsis*, warmth and long days; in Atlantic salmon, long photoperiod). Winter-dependent
135 genes are therefore intrinsically linked to unidirectional smolt development, and may play a

136 mechanistic role in pre-adaptation of the gill for seawater migration. Surprisingly, canonical
137 markers of smolt status, including the reciprocal expression of NKA subunits, are not winter
138 dependent, meaning that their expression is passive to photoperiod rather than life history
139 progression[29].

140 Using our RNAseq dataset we identified novel, winter dependent genes. Next, we
141 mined our snRNAseq dataset to identify the cell clusters that express these factors (Figure S1).
142 Of particular interest was Cuzd1, a gene associated with carcinogenesis, whose expression
143 was tightly localized to non-differentiated cells [31]. We also identified Rhag, an ammonium
144 transporter thought to be erythrocyte specific in mammals, but here predominantly expressed
145 in the vascular cell (VC 3) cluster [32]; and Hg2a (CD74) a ubiquitously expression multi-
146 functional protein linked to immune defense [33]. Taken together our data show that
147 smoltification engages all gill cells in diverse regulatory phenotypes.

148 **Cell cluster-specific expression of seawater transfer-associated factors**

149 Smoltification manifests when the Atlantic salmon smolts migrate downstream and arrive in
150 the marine environment, thereby committing to an oceanic life [1]. To gain insight into this
151 critical step we compared RNA profiles of gill samples between smolts in freshwater and 24h
152 in seawater using whole gill RNAseq, identifying 144 induced and 107 suppressed genes
153 (FDR<0.01). Gene ontologies showed that the induced gene cohort was significantly
154 associated with keratinization, whereas the suppressed gene cohort related to immune
155 function (Figure 4A). We cross-referenced our whole gill RNAseq data against our snRNAseq
156 data to isolate cell-type specificity of gene expression. These data highlight the restricted
157 expression of key up-regulated genes (Figure 4B). For example, we localize the expression of
158 an enzyme involved in both ionic and acid/base balance, carbonic anhydrase, to MRCs [34,35].

159 We also show that ATP-binding cassette sub-family A member 12 (Abca12), a gene important
160 in epidermal lipid barrier formation [36], is broadly expressed, but particularly concentrated in
161 MRCs (SW), pavement, vascular, and non-differentiated cells. Interestingly, we show that a
162 protein chaperone that helps regulate chromatin state, nucleoplasmin [37,38], is expressed
163 specifically in non-differentiated, vascular and pavement cells groups, suggesting that these
164 cell types undergo a change in chromatin status under seawater exposure.

165 **Conclusions**

166 Our results bring insightful cellular resolution to the complexity of the Atlantic salmon gill and
167 the compositional changes that occur during smoltification. Of particular interest was the
168 suppression of immune cell types, which correlates with reduction in immune-related genes
169 and suppression of immune function during smoltification [39–41]. These data are a puzzle. The
170 marine environment is awash with parasites, bacteria and viruses to which the salmon is
171 potentially vulnerable, so loss of immune function would make little sense. Future work
172 should focus on why and how the immune system is affected in aquaculture. Conceivably
173 these data point towards an adaptive immunological reprogramming that helps to avoid
174 immune shock when the salmon transition between the distinctive pathogen complements of
175 fresh- and seawater habitats [42,43]. Alternatively, artificial smolt production may drive abnormal
176 immunosuppression. The constant light routinely used to stimulate smolts would profoundly
177 undermine the immune defenses of mammals *via* disruption of the circadian clock [44].

178 Our data also shows that smoltification-driven transcriptional regulation occurs not
179 only in MRCs and ACs, but also in other distinctive cell types including pavement cells, vascular
180 cells and non-differentiated cells. We anticipate that novel gene function within the context

181 of cell function will be a priority for future investigation, and will be assisted by the novel suite
182 of marker genes which we present here.

183

184 **References**

185 1. Stefansson, S. O., Björnsson, B. T., Ebbesson, L. O. E. & McCormick, S. D.
186 Smoltification. in *Fish Larval Physiology* 639–681 (2008).

187 2. Strand, J. E. T., Hazlerigg, D. & Jørgensen, E. H. Photoperiod revisited: is there a critical
188 day length for triggering a complete parr–smolt transformation in Atlantic salmon
189 Salmo salar? *J. Fish Biol.* **93**, 440–448 (2018).

190 3. Evans, D. H., Piermarini, P. M. & Choe, K. P. The multifunctional fish gill: Dominant site
191 of gas exchange, osmoregulation, acid-base regulation, and excretion of nitrogenous
192 waste. *Physiol. Rev.* **85**, 97–177 (2005).

193 4. Koppang, E. O. *et al.* Salmonid T cells assemble in the thymus, spleen and in novel
194 interbranchial lymphoid tissue. *J. Anat.* **217**, 728–739 (2010).

195 5. Wilson, J. M. & Laurent, P. Fish gill morphology: Inside out. *J. Exp. Zool.* **293**, 192–213
196 (2002).

197 6. Laurent, P. & Dunel-Erb, S. *The Pseudobranch: Morphology and Function*. *Fish*
198 *Physiology* vol. 10 (1984).

199 7. Newstead, J. D. Fine structure of the respiratory lamellae of teleostean gills. *Zeitschrift*
200 *für Zellforsch. und Mikroskopische Anat.* **79**, 396–428 (1967).

201 8. Rojo, M. C., Blánquez, M. J. & González, M. E. A histochemical study of the distribution

202 of lectin binding sites in the developing branchial area of the trout Salmo trutta. *J.*
203 *Anat.* **189**, 609–621 (1996).

204 9. Laurent, P., Dunel-Erb, S., Chevalier, C. & Lignon, J. Gill epithelial cells kinetics in a
205 freshwater teleost, Oncorhynchus mykiss during adaptation to ion-poor water and
206 hormonal treatments. *Fish Physiol. Biochem.* **13**, 353–370 (1994).

207 10. Dunel-Erb, S., Chevalier, C. & Laurent, P. Distribution of neuroepithelial cells and
208 neurons in the trout gill filament: comparison in spring and winter. *Can. J. Zool.* **72**,
209 1794–1799 (1994).

210 11. Hootman, S. R. & Philpott, C. W. Accessory cells in teleost branchial epithelium. *Am. J.*
211 *Physiol. - Regul. Integr. Comp. Physiol.* **7**, (1980).

212 12. Mccormick, S. D., Regish, A. M., Christensen, A. K. & Björnsson, B. T. Differential
213 regulation of sodium – potassium pump isoforms during smolt development and
214 seawater exposure of Atlantic salmon. 1142–1151 (2013) doi:10.1242/jeb.080440.

215 13. Sardet, C., Pisam, M. & Maetz, J. The surface epithelium of teleostean fish gills. *J. Cell*
216 *Biol.* **80**, 96–117 (1979).

217 14. Edwards, S. L., Tse, C. M. & Toop, T. Immunolocalisation of NHE3-like
218 immunoreactivity in the gills of the rainbow trout (Oncorhynchus mykiss) and the
219 blue-throated wrasse (Pseudolabrus tetrious). *J. Anat.* **195**, 465–469 (1999).

220 15. Yan, J. J., Chou, M. Y., Kaneko, T. & Hwang, P. P. Gene expression of Na+/H+
221 exchanger in zebrafish H+-ATPase-rich cells during acclimation to low-Na+ and acidic
222 environments. *Am. J. Physiol. - Cell Physiol.* **293**, 1814–1823 (2007).

223 16. Hirata, T. *et al.* Mechanism of acid adaptation of a fish living in a ph 3.5 lake. *Am. J.*

224 *Physiol. - Regul. Integr. Comp. Physiol.* **284**, (2003).

225 17. Hiroi, J., McCormick, S. D., Ohtani-Kaneko, R. & Kaneko, T. Functional classification of
226 mitochondrion-rich cells in euryhaline Mozambique tilapia (Oreochromis
227 mossambicus) embryos, by means of triple immunofluorescence staining for Na+/K+-
228 ATPase, Na +/K+/2Cl- cotransporter and CFTR anion channel. *J. Exp. Biol.* **208**, 2023–
229 2036 (2005).

230 18. Hiroi, J., Yasumasu, S., McCormick, S. D., Hwang, P. P. & Kaneko, T. Evidence for an
231 apical Na-Cl cotransporter involved in ion uptake in a teleost fish. *J. Exp. Biol.* **211**,
232 2584–2599 (2008).

233 19. Tang, C. H., Hwang, L. Y. & Lee, T. H. Chloride channel CLC-3 in gills of the euryhaline
234 teleost, tetraodon nigroviridis: Expression, localization and the possible role of
235 chloride absorption. *J. Exp. Biol.* **213**, 683–693 (2010).

236 20. Preest, M. R., Gonzalez, R. J. & Wilson, R. W. A pharmacological examination of Na+
237 and Cl- transport in two species of freshwater fish. *Physiol. Biochem. Zool.* **78**, 259–
238 272 (2005).

239 21. Marshall, W. S., Lynch, E. M. & Cozzi, R. R. F. Redistribution of immunofluorescence of
240 CFTR anion channel and NKCC cotransporter in chloride cells during adaptation of the
241 killifish Fundulus heteroclitus to sea water. *J. Exp. Biol.* **205**, 1265–1273 (2002).

242 22. Evans, D. H. Freshwater fish gill ion transport: August Krogh to morpholinos and
243 microprobes. *Acta Physiol. (Oxf).* **202**, 349–359 (2011).

244 23. Lorgen, M. *et al.* Functional divergence of type 2 deiodinase paralogs in the Atlantic
245 salmon. *Curr. Biol.* **25**, 936–941 (2015).

246 24. Stuart, T. *et al.* Comprehensive Integration of Single-Cell Data. *Cell* **177**, 1888-
247 1902.e21 (2019).

248 25. Leguen, I., Le Cam, A., Montfort, J., Peron, S. & Fautrel, A. Transcriptomic analysis of
249 trout gill ionocytes in fresh water and sea water using laser capture microdissection
250 combined with microarray analysis. *PLoS One* **10**, 1–22 (2015).

251 26. Boyle, D., Clifford, A. M., Orr, E., Chamot, D. & Goss, G. G. Mechanisms of Cl- uptake in
252 rainbow trout: Cloning and expression of slc26a6, a prospective Cl-/HCO3- exchanger.
253 *Comp. Biochem. Physiol. -Part A Mol. Integr. Physiol.* **180**, 43–50 (2015).

254 27. Saha, D. *et al.* Hemoglobin Expression in Nonerythroid Cells: Novel or Ubiquitous? *Int.*
255 *J. Inflam.* **2014**, (2014).

256 28. Koppang, E. O., Kvellestad, A. & Fischer, U. *Mucosal Health in Aquaculture Fish*
257 *mucosal immunity: gill*. *Mucosal Health in Aquaculture* (Elsevier Inc., 2015).
258 doi:10.1016/B978-0-12-417186-2/00005-4.

259 29. Iversen, M. *et al.* RNA profiling identifies novel, photoperiodhistory dependent
260 markers associated with enhanced saltwater performance in juvenile Atlantic salmon.
261 *PLoS One* **15**, 1–21 (2020).

262 30. Song, J., Angel, A., Howard, M. & Dean, C. Vernalization - a cold-induced epigenetic
263 switch. *J. Cell Sci.* **125**, 3723–3731 (2012).

264 31. Liaskos, C., Rigopoulou, E. I., Orfanidou, T., Bogdanos, D. P. & Papandreou, C. N.
265 CUZD1 and Anti-CUZD1 Antibodies as Markers of Cancer and Inflammatory Bowel
266 Diseases. **2013**, (2013).

267 32. Tilley, L. *et al.* A new blood group system , RHAG : three antigens resulting from amino

268 acid substitutions in the Rh-associated glycoprotein. 151–159 (2010)
269 doi:10.1111/j.1423-0410.2009.01243.x.

270 33. Su, H., Na, N., Zhang, X. & Zhao, Y. The biological function and significance of CD74 in
271 immune diseases. *Inflamm. Res.* **66**, 209–216 (2017).

272 34. Houde, A. L. S. *et al.* Salmonid gene expression biomarkers indicative of physiological
273 responses to changes in salinity and temperature, but not dissolved oxygen. *J. Exp.*
274 *Biol.* **222**, (2019).

275 35. Zbanyszek, R. & Smith, L. S. Changes in carbonic anhydrase activity in coho salmon
276 smolts resulting from physical training and transfer into seawater. *Comp. Biochem.*
277 *Physiol. -- Part A Physiol.* **79**, 229–233 (1984).

278 36. Akiyama, M. The roles of ABCA12 in epidermal lipid barrier formation and
279 keratinocyte differentiation. *Biochim. Biophys. Acta - Mol. Cell Biol. Lipids* **1841**, 435–
280 440 (2014).

281 37. Bouleau, A. *et al.* Maternally inherited npm2 mRNA is crucial for egg developmental
282 competence in zebrafish. *Biol. Reprod.* **91**, 1–9 (2014).

283 38. Chen, P. *et al.* Nucleoplasmin is a limiting component in the scaling of nuclear size
284 with cytoplasmic volume. *J. Cell Biol.* **218**, 4063–4078 (2019).

285 39. Jensen, I., Overrein, M. C., Fredriksen, B. N., Strandskog, G. & Seternes, T. Differences
286 in smolt status affect the resistance of Atlantic salmon (Salmo salar L.) against
287 infectious pancreatic necrosis, while vaccine-mediated protection is unaffected. *J. Fish*
288 *Dis.* **42**, 1271–1282 (2019).

289 40. Johansson, L. H., Timmerhaus, G., Afanasyev, S., Jørgensen, S. M. & Krasnov, A.

290 Smoltification and seawater transfer of Atlantic salmon (Salmo salar L.) is associated
291 with systemic repression of the immune transcriptome. *Fish Shellfish Immunol.* **58**,
292 33–41 (2016).

293 41. Nuñez-Ortiz, N. *et al.* Atlantic salmon post-smolts adapted for a longer time to
294 seawater develop an effective humoral and cellular immune response against
295 Salmonid alphavirus. *Fish Shellfish Immunol.* **82**, 579–590 (2018).

296 42. Lee, S.-Y. & Eom, Y.-B. Analysis of Microbial Composition Associated with Freshwater
297 and Seawater. *Biomed. Sci. Lett.* **22**, 150–159 (2016).

298 43. Wang, Y. *et al.* Comparison of the levels of bacterial diversity in freshwater, intertidal
299 wetland, and marine sediments by using millions of illumina tags. *Appl. Environ.*
300 *Microbiol.* **78**, 8264–8271 (2012).

301 44. Scheiermann, C., Gibbs, J., Ince, L. & Loudon, A. Clocking in to immunity. *Nature*
302 *Reviews Immunology* vol. 18 423–437 (2018).

303 45. Matson, K. J. E. *et al.* Isolation of adult spinal cord nuclei for massively parallel single-
304 nucleus RNA sequencing. *J. Vis. Exp.* **2018**, 1–12 (2018).

305 **<u>Material and Methods</u>**

306 **Animal welfare statement**

307 The Atlantic salmon smoltification experiment was conducted as part of the routine, smolt
308 production at Kårvik havbruksstasjonen, approved by the Norwegian Animal Research
309 Authority (NARA) for the maintenance of stock animals for experiments on salmonids. This is
310 in accordance with Norwegian and European legislation on animal research.

311 **Experimental Design**

312 Atlantic salmon (*Salmo salar*, Aquagene commercial stain) were raised from hatching in
313 freshwater, under continuous light (LL, > 200 lux at water surface) at ambient temperature
314 (~10°C). Juvenile salmon were housed in 500 L circular tanks and fed continuously with
315 pelleted salmon feed (Skretting, Stavanger, Norway). At seven months of age parr (mean
316 weight 49.5g) were sampled for T1 (experiment start). Two days later remaining parr were
317 equally distributed between two 100L circular tanks, and over the next seven days the
318 photoperiod was incrementally reduced to a short photoperiod (SP, 8h light:16h darkness). T2
319 sampling occurred on experimental day 53 (44 days on SP), remaining parr were transferred
320 back to LL on experimental day 60. T3 sampling occurred on experimental day 110 (50 days
321 after return to LL), then a sub-cohort of fish were netted out and transferred to full strength
322 seawater for 24h before the final T4 collection.

323 **RNAseq Analysis**

324 Gill samples were collected, RNA extracted and libraries prepared, sequenced and mapped as
325 Iversen et al (2020). Raw counts were analysed using EdgeR (ver. 3.30.0), using R (ver. 4.0.2)
326 and RStudio (ver. 1.1.456). An ANOVA-like test was used to identify differential expressed
327 genes between T1-T3 samples. Clustering analysis was performed using Pearson correlation,
328 and heapmaps rendered using the R package pheatmap. An exact test was performed to
329 identify differential expressed genes between T3 and T4.

330 **Single nuclei RNAseq Analysis**

331 Gills for single nuclei analysis were collected on dry ice and stored at -80°C. Duplcate samples
332 were processed for T1-T4. Nuclei were released by detergent mechanical lysis, then samples
333 were homogenized (30s) and nuclei isolated by sucrose gradient [45]. Libraries were created

334 using Chromium Single Cell 3' GEM, Library & Gel Bead Kit v3 (10x technologies) by University
335 of Manchester genomic technology core facility (UK). Raw data was converted to counts per
336 cell using Cell Ranger (10x Technologies, ver. 3.1.0) and processed using NCBI annotations.
337 The R package Seurat (ver. 3.1.5) was used to perform an integrated analysis using all
338 snRNAseq data [24], further details in results and discussion. Raw data will be available following
339 peer-reviewed publication.

340

341 **Acknowledgements**

342 The authors thank all of the animal staff at Kårvik havbruksstasjonen for their expert care of
343 the research animals, and the University of Manchester Genomics Technology core facility
344 (UK) for performing chromium 10x library preparation for snRNAseq. ACW is supported by the
345 Tromsø forskningsstiftelse (TFS) grant awarded to DGH (TFS2016DH). The Sentinel North
346 Transdisciplinary Research Program Université Laval and UiT awarded to DGH supports this
347 work. SHW is supported a grant from the Tromsø forskningsstiftelse (TFS) starter grant
348 TFS2016SW. Experimental costs were covered by HFSP grant "Evolution of seasonal timers"
349 RGP0030 /2015 awarded to ASIL and DGH.

350

351 **Author Contributions**

352 Conceptualization, A.C.W., Y.M., E.H.J., A.S.I.L and D.G.H; Resources, A.C.W, Y.M and M.I.;
353 Investigation, A.C.W., Y.M., M.I. E.H.J and D.G.H; Formal Analysis, A.C.W, Y.M., L.I., T.N and
354 S.R.S; Visualization, A.C.W and S.H.W; Writing – Original Draft, A.C.W and S.H.W; Writing –

355 Review & Editing, All; Supervision, A.S.I.L and D.G.H; Project Administration, A.S.I.L and D.G.H;
356 Funding Acquisition, A.S.I.L and D.G.H.

357

358 **Figure Legends**

359 **Figure 1.** Single nuclei RNAseq analysis of Atlantic salmon gill tissue. A) Gill tissue processing.
360 B) UMAP plot of pooled cell data from 18844 cells representing eight samples from four
361 collection states. The plot indicates 20 separate cell clusters. C) Expression of marker genes in
362 20 cell clusters. From left to right: hierarchical relatedness of difference cell clusters; total cells
363 in each cluster; UMI number in each cell cluster; gene features in each cell cluster; violin plots
364 showing expression pattern of marker genes for each cluster. Abbreviations: ACs - accessory
365 cells, DCs - dendritic cells, ECs - epithelial cells, fib - fibrocytes, GCs - goblet cells, LECs -
366 lymphatic endothelial cells, MCs - myeloid cells, MRC - mitochondrion-rich cells, NDCs - non-
367 differentiated cells, PVCs, pavement cells, RBCs - red blood cells (erythrocytes), TCs - T cells,
368 VCs - vascular cells.

369 **Figure 2.** Comparative abundance of cell clusters at different sampling points. A) Experimental
370 design. Fish were kept in constant light (LL) from hatching then transferred to short
371 photoperiod (SP; 8L:16D) for 8 weeks before being returned to constant light (LL) for 8 weeks.
372 Finally the fish were transferred to sea water for 24h. Sample points are indicated T1-T4. B)
373 Subset of cell clusters from T2, T3 and T4 (green and red dots) overlaid on T1 cells (grey dots).
374 C) Increasing abundance of sea-water mitochondrion-rich cells (MRCs SW) and vascular cells
375 (VC 3) during smoltification C) Decreasing abundance of leukocytes and immune-associated
376 cells during smoltification.

377 **Figure 3.** Photoperiodic changes in gill gene expression and localized cell cluster expression.
378 A) Heat map representing 9746 genes differentially regulated (FDR <0.01) from T1-T3.
379 Regulatory patterns for 5 major cluster are shown as amplitude index and 95% confidence
380 limits. Major gene ontology terms for each cluster are shown. B) RNAseq data for "classical"
381 smoltification-related genes and violin plots showing their cluster specific expression.

382 **Figure 4.** Sea-water transfer-associated changes in gill gene expression and localized cell
383 cluster expression. A) Heat map representing 253 genes differentially regulated (FDR <0.01)
384 by 24h seawater transfer. Major gene ontology terms for each cluster are shown. B) RNAseq
385 data for sea-water transfer-related genes and violin plots showing their cluster specific
386 expression.

387 **Supplemental Figure 1.** RNAseq data for winter-dependent genes and violin plots showing
388 their cluster specific expression.

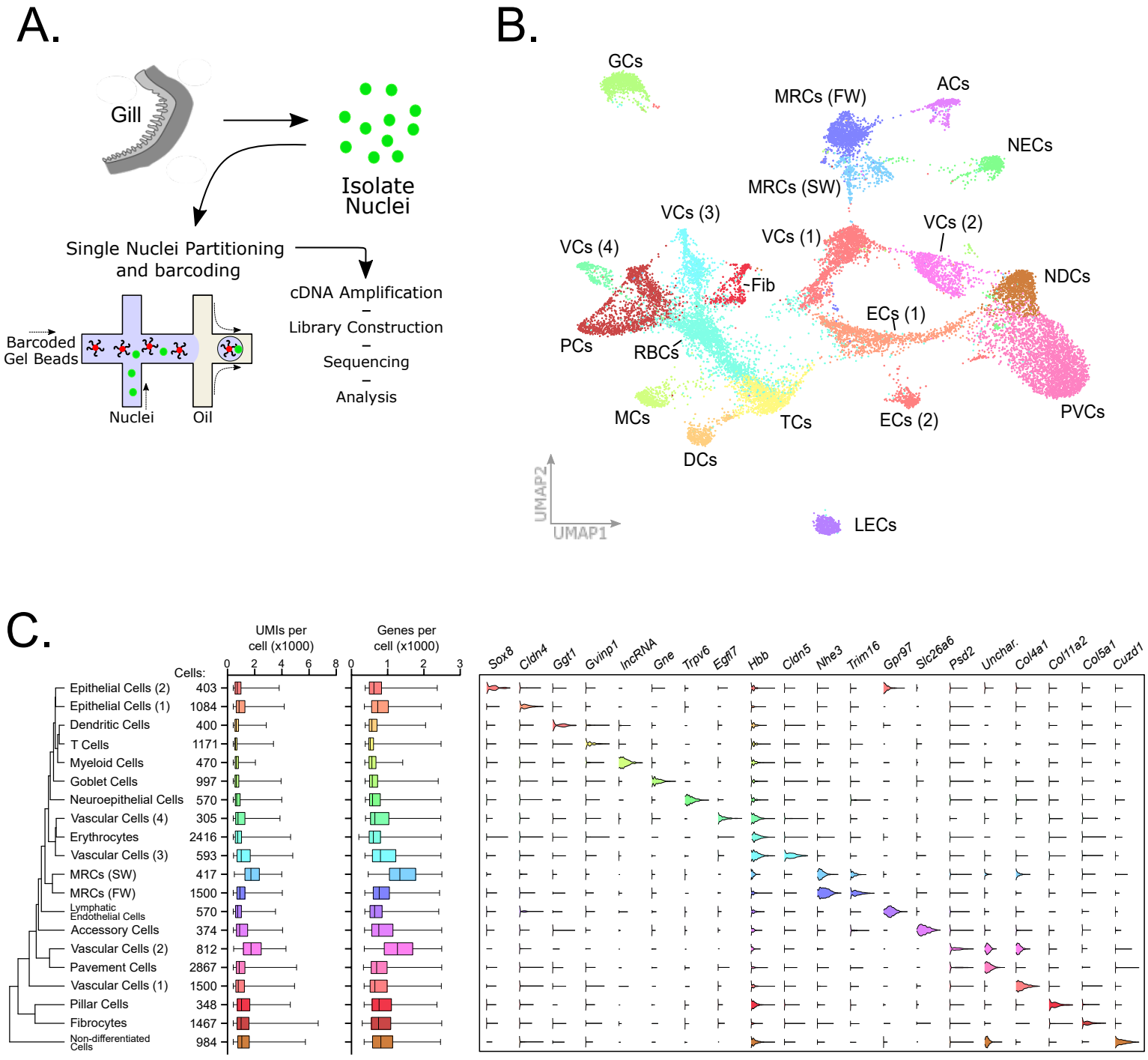
A.
Gill
Isolate Nuclei
Single Nuclei Partitioning and barcoding
cDNA Amplification
Library Construction
Sequencing
Analysis
Barcoded Gel Beads
Nuclei
Oil
B.
GCs
MRCs (FW)
ACs
NECs
MRCs (SW)
VCs (3)
VCs (1)
VCs (2)
VCs (4)
Fib
NDCs
ECs (1)
PCs
RBCs
MCs
TCs
ECs (2)
PVCs
DCs
UMAP2
UMAP1
LECs
C.
UMIs per cell (x1000)
Genes per cell (x1000)
Cells:
Epithelial Cells (2) 403
Epithelial Cells (1) 1084
Dendritic Cells 400
T Cells 1171
Myeloid Cells 470
Goblet Cells 997
Neuroepithelial Cells 570
Vascular Cells (4) 305
Erythrocytes 2416
Vascular Cells (3) 593
MRCs (SW) 417
MRCs (FW) 1500
Lymphatic Endothelial Cells 570
Accessory Cells 374
Vascular Cells (2) 812
Pavement Cells 2867
Vascular Cells (1) 1500
Pillar Cells 348
Fibrocytes 1467
Non-differentiated Cells 984
Sox8
Cldn4
Ggt1
Gvinp1
lncRNA
Gne
Trpv6
Egfl7
Hbb
Cldn5
Nhe3
Trim16
Gpr97
Slc26a6
Psd2
Unchar.
Col4a1
Col11a2
Col5a1
Cuzd1

Figure 1.

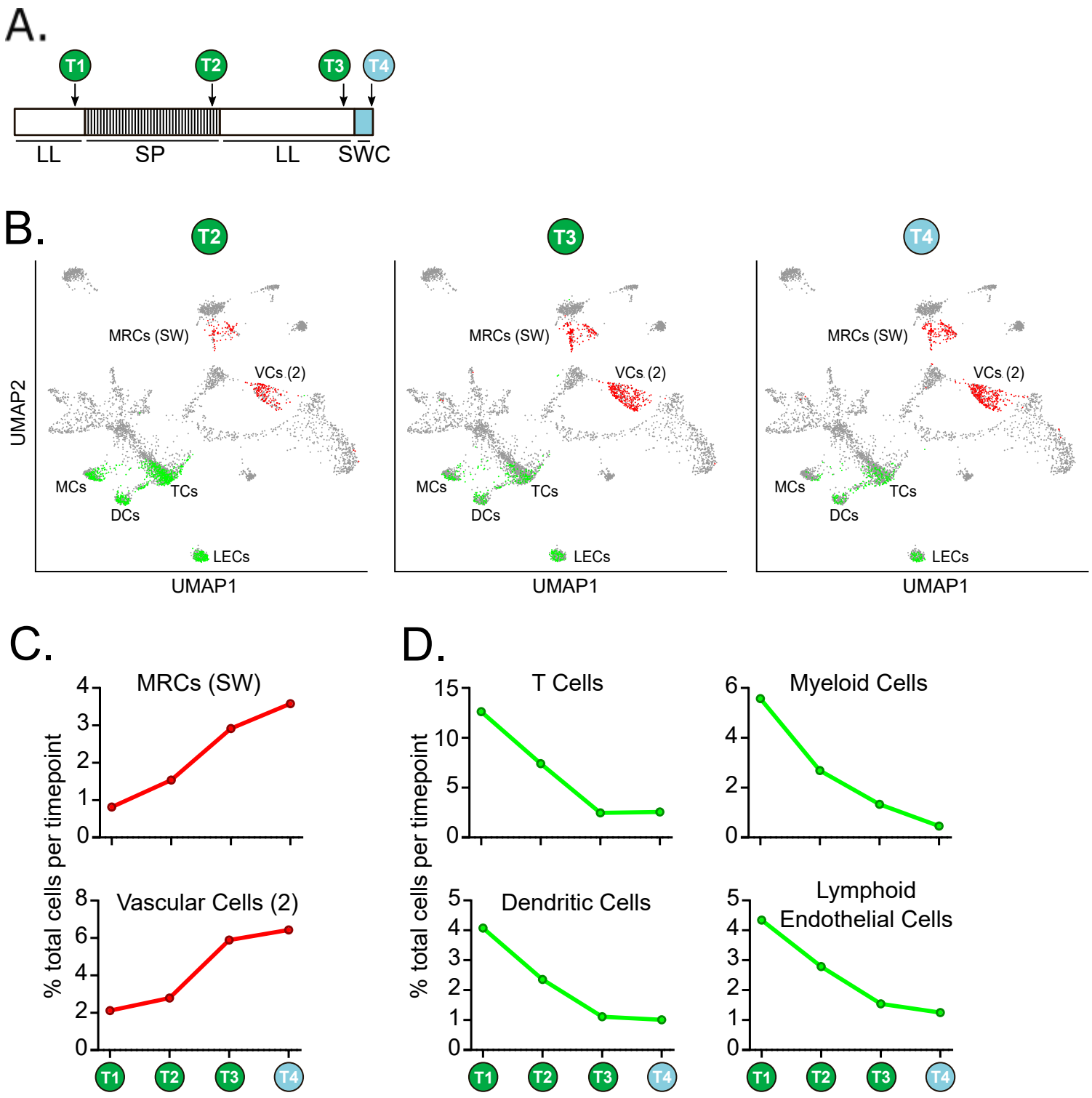
A.
T1
T2
T3
T4
LL
SP
LL
SWC
B.
T2
T3
T4
MRCs (SW)
VCs (2)
MCs
TCs
DCs
LECs
UMAP2
UMAP1
C.
MRCs (SW)
Vascular Cells (2)
% total cells per timepoint
D.
T Cells
Myeloid Cells
Dendritic Cells
Lymphoid Endothelial Cells

Figure 2.

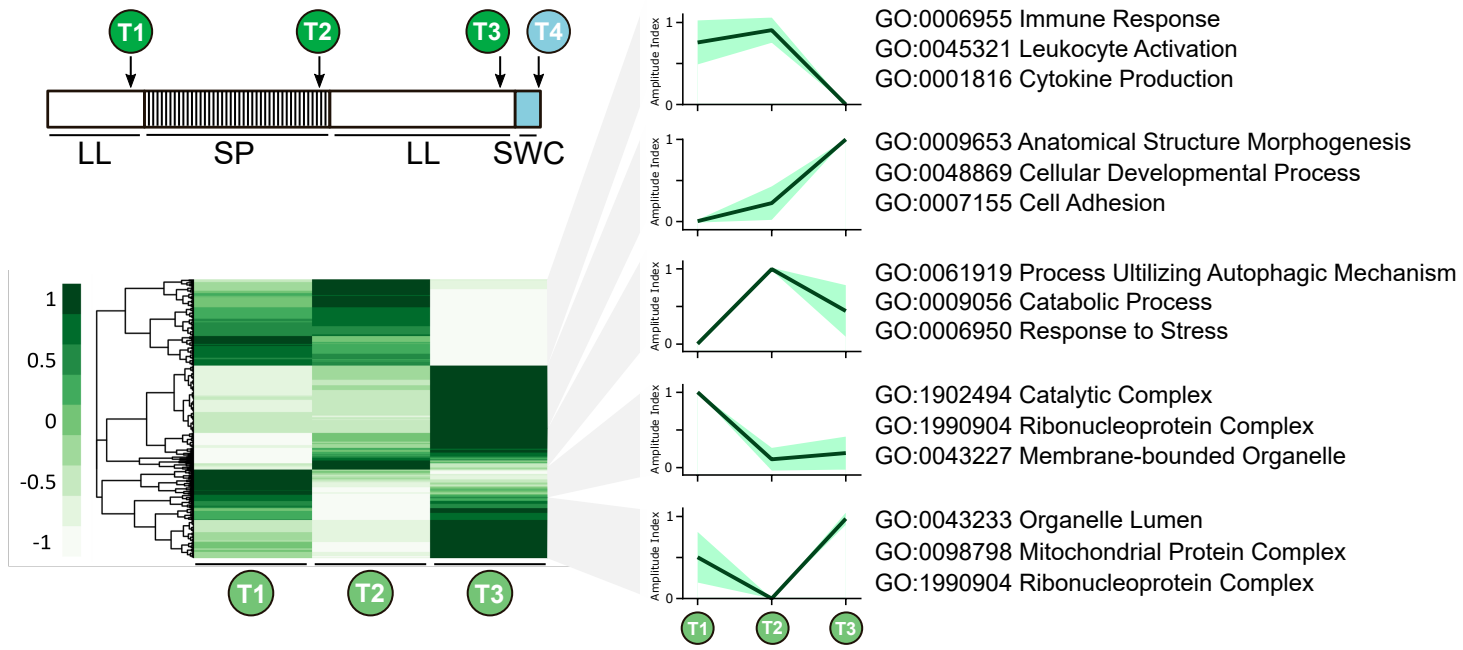
A.
T1
T2
T3
T4
LL
SP
LL
SWC
1
0.5
0
-0.5
-1
T1
T2
T3
Amplitude Index
GO:0006955 Immune Response
GO:0045321 Leukocyte Activation
GO:0001816 Cytokine Production
GO:0009653 Anatomical Structure Morphogenesis
GO:0048869 Cellular Developmental Process
GO:0007155 Cell Adhesion
GO:0061919 Process Ultilizing Autophagic Mechanism
GO:0009056 Catabolic Process
GO:0006950 Response to Stress
GO:1902494 Catalytic Complex
GO:1990904 Ribonucleoprotein Complex
GO:0043227 Membrane-bounded Organelle
GO:0043233 Organelle Lumen
GO:0098798 Mitochondrial Protein Complex
GO:1990904 Ribonucleoprotein Complex

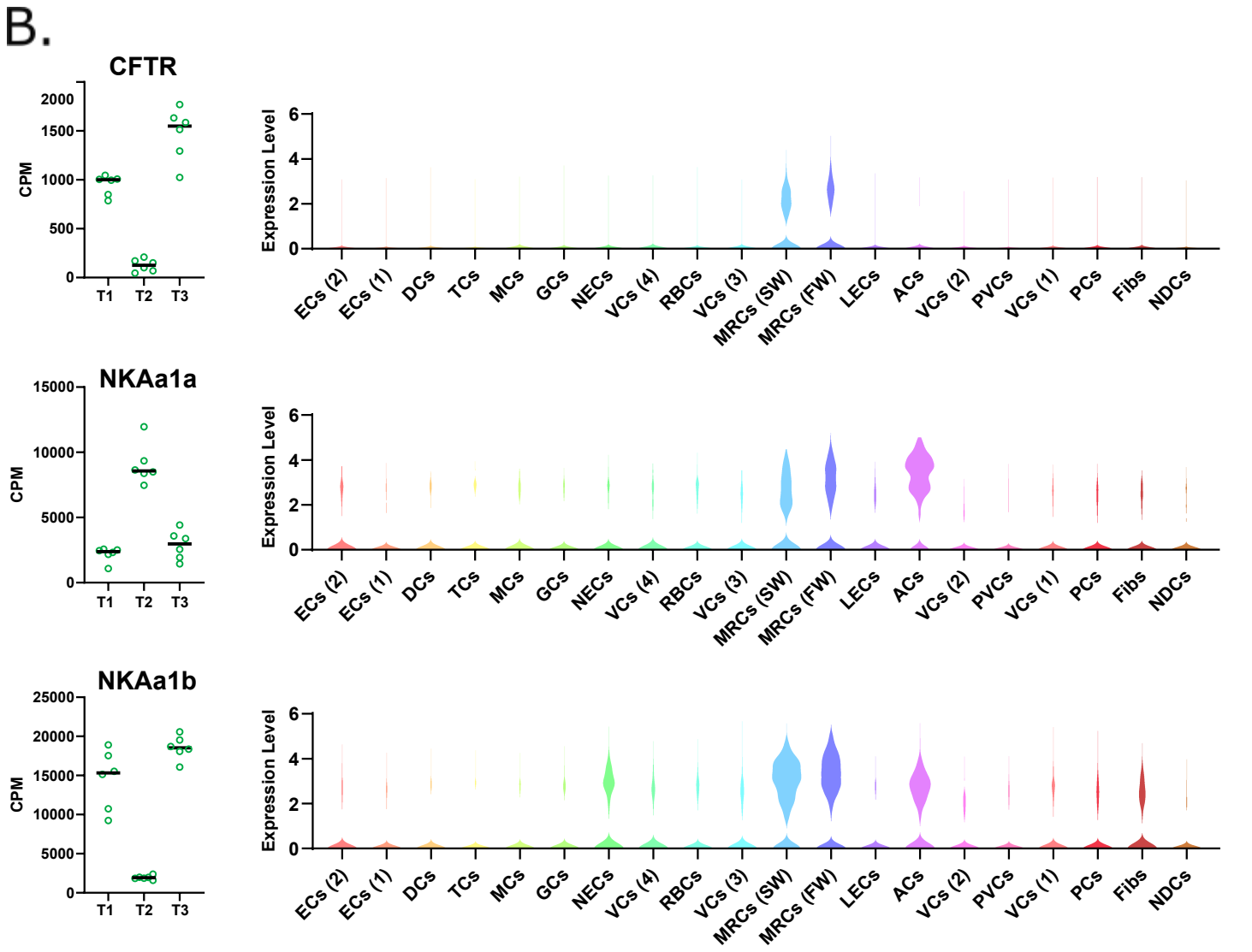
B.
CFTR
NKAa1a
NKAa1b
CPM
Expression Level
T1
T2
T3
ECs (2)
ECs (1)
DCs
TCs
MCs
GCs
NECs
VCs (4)
RBCs
VCs (3)
MRCs (SW)
MRCs (FW)
LECs
ACs
VCs (2)
PVCs
VCs (1)
PCs
Fibs
NDCs

Figure 3.

A.

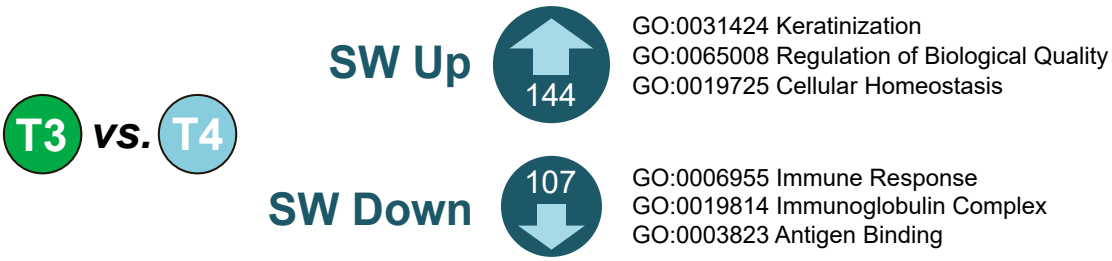
T3
vs.
T4
SW Up
144
GO:0031424 Keratinization
GO:0065008 Regulation of Biological Quality
GO:0019725 Cellular Homeostasis
SW Down
107
GO:0006955 Immune Response
GO:0019814 Immunoglobulin Complex
GO:0003823 Antigen Binding

B.

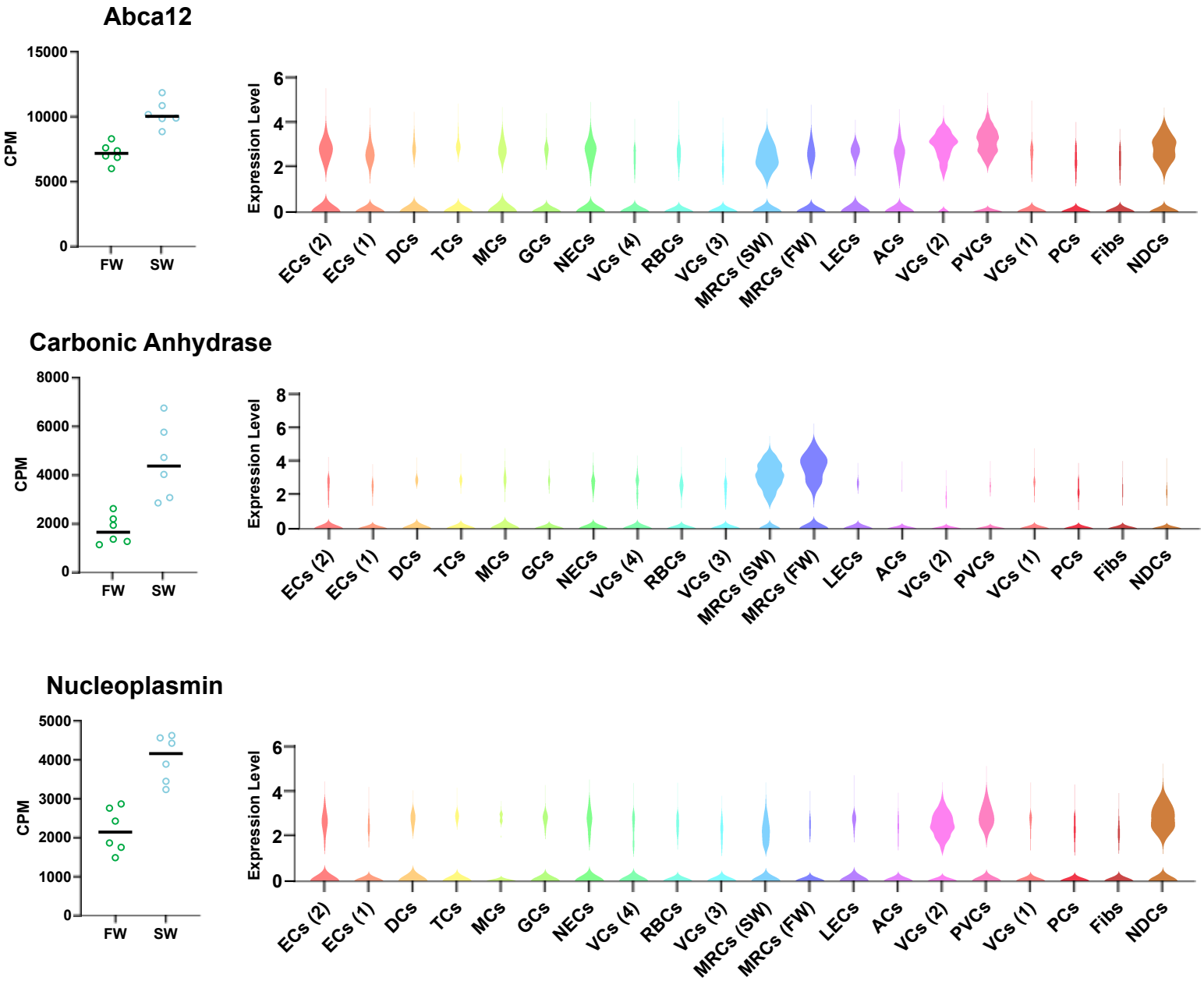
Abca12
CPM
15000
10000
5000
0
FW
SW
Expression Level
6
4
2
0
ECs (2)
ECs (1)
DCs
TCs
MCs
GCs
NECs
VCs (4)
RBCs
VCs (3)
MRCs (SW)
MRCs (FW)
LECs
ACs
VCs (2)
PVCs
VCs (1)
PCs
Fibs
NDCs
Carbonic Anhydrase
CPM
8000
6000
4000
2000
0
FW
SW
Expression Level
8
6
4
2
0
ECs (2)
ECs (1)
DCs
TCs
MCs
GCs
NECs
VCs (4)
RBCs
VCs (3)
MRCs (SW)
MRCs (FW)
LECs
ACs
VCs (2)
PVCs
VCs (1)
PCs
Fibs
NDCs
Nucleoplasmin
CPM
5000
4000
3000
2000
1000
0
FW
SW
Expression Level
6
4
2
0
ECs (2)
ECs (1)
DCs
TCs
MCs
GCs
NECs
VCs (4)
RBCs
VCs (3)
MRCs (SW)
MRCs (FW)
LECs
ACs
VCs (2)
PVCs
VCs (1)
PCs
Fibs
NDCs

Figure 4.